Eur Biophys J (1994) 23: 361–368

European Biophysics Journal

Intermediate states in ligand photodissociation of carboxymyoglobin studied by dispersive X-ray absorption

S. Della Longa[1], **I. Ascone**[2], **A. Fontaine**[2], **A. Congiu Castellano**[3], **A. Bianconi**[3]

[1] Dipartimento di Medicina Sperimentale, Università dell'Aquila, v. S. Sisto 20, I-67100 L'Aquila, Italy
(Tel.: +39 862 433568, Fax: +39 862 433523, e-mail: DELLALONGA@VAXAQ.CC.UNIVAQ.IT)
[2] LURE (Lab. CNRS, CEA, MEN) Bat. 209D, F-91405 Orsay, France
[3] Dipartimento di Fisica, Università di Roma "La Sapienza", P.le A. Moro 5, I-00185 Roma, Italy

Received: 13 May 1994 / Accepted in revised form: 2 August 1994

Abstract. The ligand photodissociation of sperm whale carboxymyoglobin (MbCO) at low temperature (15 K–100 K) under extended illumination has been studied by X-ray Absorption Near Edge Structure (XANES) spectroscopy using the dispersive technique. XANES simulations through the multiple scattering (MS) approach allow one to interpret the spectroscopic data in structural terms, and to investigate the Fe site structure configurations of the states that follow the CO photodissociation as a function of temperature. The Fe site in the photoproduct is unbound, with an overall structure similar to the deoxy-form (Mb) of the protein. The Fe site structure changes from $T < 30$ K (Mb*) to $T > 50$ K (Mb**), revealing the existence of a slower unbound state Mb**. A model is proposed which includes the faster state (Mb*) as a planar porphyrin ring with a displacement of Fe from the heme plane of less than 0.3 Å, and the slower state (Mb**) with a domed heme.

Key words: Hemoproteins – Synchrotron radiation – XANES – Photolysis

Introduction

Myoglobin is a standard system for protein dynamics studies: a growing set of experimental data confirms the existence, inside a main structural protein state, of different substates (Parak et al. 1987; Frauenfelder et al. 1988; Doster et al. 1989a). The various conformations of both bound and unbound myoglobin substates are expected to control the ligand binding kinetics, depending on several factors, such as protein sequence, solvent, pH, temperature.

An important goal in protein dynamics of myoglobin is to get a satisfactory description of i) the conformational landscape of the different equilibrium forms of the protein (e.g. bound MbCO and unbound Mb) and ii) the structural intermediates in the ligand binding process.

Correspondence to: S. Della Longa

The conformational landscape of MbCO begins to be understood through the definition of a single conformational coordinate, the Fe–C–O angle. Fourier transform infrared (FTIR) spectroscopy studies (Ormos et al. 1988) of MbCO have identified three CO stretching frequency bands, A_0, A_1 and A_3 in sperm whale, which can be related, through their linear dichroism in partial photolysis experiments (Moore et al. 1988), to the CO tilting angle α from the heme normal, resulting in $\alpha(A_0) = 15° \pm 10°$, $\alpha(A_1) = 28° \pm 2°$, $\alpha(A_3) = 33° \pm 4°$. Each band after photolysis exhibits a different non-exponential rebinding. The existence of conformational substates explains why these processes are non-exponential in time. Hence the A_n bands probe the three main substates of tier 0 of the ground state. Inhomogeneity of myoglobin at low temperature (each molecule possessing a different tertiary structure and CO binding rate coefficient) has been demonstrated by multiple flash experiments (Austin et al. 1975) confirming the importance of defining a conformational coordinate. The Fe–C–O angle is certainly a good probe of the functionally important conformations at the Fe site; however the existence of other Fe coordination geometries, that bind the CO molecule giving the same bond angle, cannot be excluded.

On the other hand, the conformational landscape of deoxy myoglobin Mb is still unclear. In a recent FTIR study (Mourant et al. 1993), a characterisation of the photo product states was reported by studying the CO stretching band B_n after flash photolysis below 100 K. However, the observed substates reflect motion of CO in the heme pocket and not conformational minima at the Fe site. Structural heterogeneity of the Fe–N_ε(His^{F8}) bond in various hemoglobin and myoglobin derivatives has been probed by a study of the Raman active iron-histidine stretching mode (Gilch et al. 1993), suggesting that this parameter is a good conformational coordinate of the unbound protein.

An insight into the conformational landscape problem is given by XANES (X-ray Absorption Near Edge Structure) spectroscopy. The XANES method is a probe of the local structure (bond angles and geometry) around the Fe site, characterised by a very fast coherence time ($\sim 10^{-15}$ s).

Since atomic motions are slower than that, it gives the iron site structure averaged over the protein ensemble, i.e. the XANES signal is close to the conformation with the highest probability. The average bending angle α of sperm whale MbCO both in solution and in the crystal was found to be about 30° (Bianconi et al. 1985 b). Moreover XANES probes the Fe site structure in the unbound Mb ensemble as well as in the MbCO ensemble.

Flash photolysis on MbCO provides a classical physical method (Iizuka et al. 1974; Austin et al. 1975; Hong et al. 1990) to investigate the ligand rebinding process. These processes have been described by a three-well model, with time-dependent barriers among three main states, each one can have many substates (scheme(1)):

$$\text{MbCO} \leftrightarrow \text{Mb}^* \leftrightarrow \text{Mb} \qquad (1)$$

where Mb* indicates the protein conformations when CO is dissociated but confined in the heme pocket, and Mb indicates the deoxy-Mb conformations when CO is in the solvent. Below about 180 K, in a 2:1 glycerol-water solvent, a single non exponential recombination process, Mb* → MbCO is reported from kinetic data (Austin et al. 1975). At such a low temperature, the ligand cannot exit the protein and the binding occurs directly from the heme pocket. Moreover, each protein molecule is frozen in its local conformational minimum and no fluctuations between substates occur (Elber and Karplus 1987). No linear dichroism of the CO stretching bands is found after photolysis, indicating that the Fe–C bond is broken and CO has moved away and is randomly oriented.

The Fe site structure of Mb and MbCO determined by both X-ray crystallography (XRD) and EXAFS (Extended X-ray Absorption Fine Structure) includes an average $Fe–N_p = 2.06$ Å in Mb and 2.01 Å in MbCO for Mb (Takano 1977; Phillips 1981; Fermi et al. 1984; Kuriyan et al. 1986; Chance et al. 1983; Powers et al. 1984, 1987; Zhang et al. 1989).

EXAFS studies carried out at low temperatures have measured the variation of the averaged distance $Fe–N_p$ between the Fe and four pyrrolic nitrogens in sperm whale carboxymyoglobin after photolysis. The experiments show that the structure of the Fe heme complex in the low temperature photo product is not completely relaxed in the Mb configuration. A distance $Fe–N_p = 2.03 \pm 0.02$ Å for Mb* in frozen solutions at 4–20 K has been reported (Powers et al. 1984). Another EXAFS study (Teng et al. 1987) reports a distance $d(Fe–N_p) = 1.98 \pm 0.02$ Å for a MbCO dried film sample, without variations of this distance after photolysis at low temperature.

On the other hand, theoretical simulations (Sassaroli and Rousseau 1986) and optical, infrared, and magnetic susceptibility studies (Fiamingo and Alben 1985) have indicated that the configuration of the heme in the Mb* photo product is very close to the fivefold Fe site configuration of Mb. Raman investigation (Rousseau and Argade 1986) of the photo product structure compared with that of Mb have shown a small expansion of the heme core size (the distance from the heme centre to the pyrrolic nitrogens, $C_t–N_p$) in the photo product.

Previous XANES studies have been performed with very low energy resolution in which the fine details of the XANES spectra were smeared out (Chance et al. 1983; Mills et al. 1984; Teng et al. 1987). We have used the dispersive method to measure fast spectra with good signal to noise ratio, and to extract structural parameters of the photo product of sperm whale myoglobin. Evidence of the existence of at least 2 substates under extended illumination at low temperature, and the definition of the average structure of the intermediate states in the ligand binding process, according to the multiple scattering (MS) theory, are reported.

Materials and methods

Carboxymyoglobin was prepared as 7 mM samples in a 2:1 glycerol-H_2O solution at pH 6.7 from sperm-whale met-myoglobin from Sigma, by standard methods described elsewhere (Antonini and Brunori 1971). A slight excess of a concentrated solution of sodium dithionite was added and finally CO was passed over the protein solution for at least 30 min just before the experiment to obtain MbCO.

The spectrometer of the dispersive line combines a focusing dispersive X-ray optical system including a triangular bent crystal and a position sensitive linear detector able to work under high flux conditions (Fontaine et al. 1989; Ascone et al. 1987). The polychromatic focus of this system, with an image size of less than 400 μm, is fixed at the sample, whereas the monochromatic focus (due to the finite size of the source) lies at about twice the distance of the polychromatic focus; here is put the array detector. This system gives high energy resolution (less than 2 eV with a Si (311) crystal) and high stability in the energy scale, because there is no mechanical movement during the data collection, so a high precision for the energy shift of the absorption edge can be obtained. A reliability better than 30 meV is achieved after temperature stabilisation of the optical system (mainly of the bent crystal). An X-ray flat fused quartz mirror at grazing incidence between the sample and the detector works as a low pass filter to remove harmonic contamination. The theoretical time scale (2.7 ms) of the dispersive technique is given by the faster frequency of the readout of the photodiode array to handle the high proton flux. Each of the 1024 sensing elements is able to transform 4×10^4 8-KeV X-ray photons into 8.8×10^7 electron-hole pairs.

The difference spectrum Mb*/MbCO was measured 'in situ', i.e. the signal recorded is always the transmitted intensity, and after two runs a difference spectrum can be obtained:

$$\Delta[\mu(E)x] = \ln[(I_{Mb^*} - I_{dark})/(I_{MbCO} - I_{dark})] \qquad (2)$$

in which I_{MbCO} and I_{Mb^*} are the transmitted X-ray intensities from the sample, before and after the illumination, at the energy E, while I_{dark} is the intensity measured without photon flux, i.e. the electronic noise (Eq. (2)). The data collection time for each spectrum was 120 s. The measured change in the optical density at the 12 eV maximum of the XANES difference spectra was $\Delta\mu = 2 \times 10^{-3}$, for a total absorption jump of 1×10^{-2}. The noise was kept lower than 2×10^{-4}. The data are presented without any manip-

ulation. The zero of the energy scale is fixed at the Fe metal K-edge defined as the first maximum of the derivative spectrum (7 111.2 eV).

The MbCO sample solution in a 1 mm thick pure aluminium cell with mylar windows, oriented perpendicular to the X-ray beam, was firstly cooled at 15 K in the dark by a liquid He close circuit cryostat, in 3 h. The temperature at the sample was probed by a carbon resistor mounted in contact with the cell. A XANES spectrum of the MbCO sample was acquired at 15 K immediately before the start of illumination. Then the sample was photolyzed by continuous illumination from a 12 V – 100 W QTH Oriel lamp model n. 6333, using optical fibre optics. Then, consecutively at each temperature (from 30 K to 100 K), further XANES measurements were collected. At 15 K, the photo product rebinds very slowly, and the time delay used is sufficient to saturate the extent of photolysis. For $T > 40$ K, the recombination becomes fast, but under continuous illumination it is possible to observe very slow states, as well as states that accumulate by optical pumping.

The photolysis results are discussed through a comparison with the XANES difference spectra between the equilibrium forms Mb and MbCO. To compare the data, we look at the spectral amplitudes normalised to the respective measured atomic absorption jump. There are two sources of error in evaluating the normalised data amplitudes: i) In the photolysis experiment, the extent of photolysis could be less than 100%, giving measured amplitudes reduced by the same percentage. The shape of the difference spectrum is expected not to depend on the extent of photolysis, while its overall amplitude does. Owing to this systematic error, the photolysis experiment gives a lower limit to the real values of the same peaks in the Mb*–MbCO spectrum. The spectra (Mb*–MbCO) for temperature $= < 30$ K were found to be unchanged after about 1 h of continuous illumination at 30 K. ii) In the data analysis of the XANES of Mb and MbCO, the fitting procedures for the subtraction of the pre-edge and normalization of the spectrum cause an error in the calculated absorption jumps, and hence in the amplitude of the XANES peaks, of a few percent. Hence it is noticeable that, within these limits, a superposition of the Mb–MbCO and Mb*–MbCO spectra is obtained between 18 eV and 38 eV (in the region of the features C1, D, D′, C2 and E of Fig. 1 and Fig. 4, see below).

The XANES simulations in real space using the full multiple scattering formalism were carried out using our G4XANES procedure, assembled by merging and extending several pre-existing programs. The procedure, described elsewhere (Della Longa et al. 1993; Li et al. 1991) has been used to perform XANES simulations on different kinds of compounds, e.g. crystals (Li et al. 1991), small molecules (Palladino et al. 1993), and low symmetry metal sites in proteins (Amiconi et al. 1989; Congiu Castellano

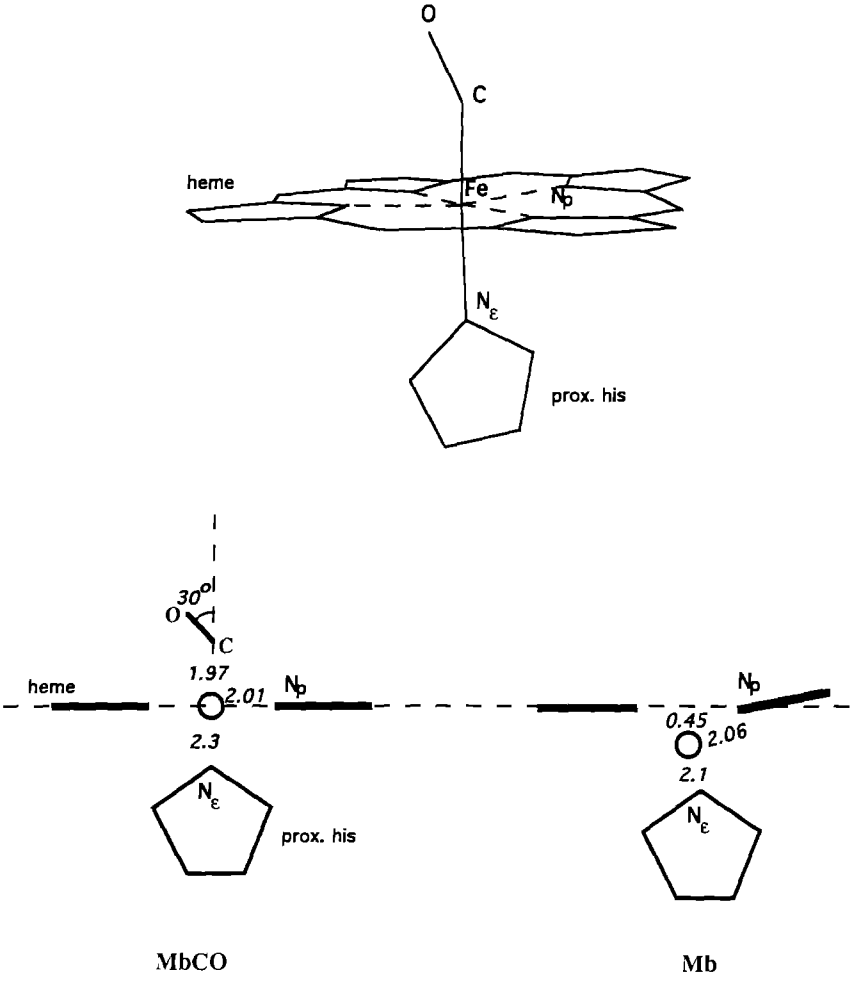

Fig. 1. *Top:* the structure of the Fe site in carboxy-myoglobin as extracted from crystallographic data (see the text). *Bottom:* sketch of the Fe site structures in MbCO and Mb as extracted from the XRD and EXAFS (see the text)

Table 1. Calculated MT parameters for MbCO

Cluster	N of atoms	Atom	Rmt (Å)	Vmt (eV)
Central atom		Fe	1.06	21.6
1 shell	1	C	0.86	21.4
	4	N	0.81	21.6
2 shell	1	O	0.83	18.4

et al. 1991; Della Longa et al. 1993). The molecular potential in the "muffin tin" (MT) form was set up by starting with an idealised MbCO cluster with a perfect planar porphyrin ring with D_{4h} symmetry and a linear Fe–C–O geometry. The molecular potential in the MT approximation has radial symmetry around each atom, up to its MT radius, and it is constant in the interstitial volume between the MT spheres, hence it is essential to minimise the discontinuities of the MT calculated potential between the atomic MT spheres. The MT radii R_{MT} for each atomic species and the value of the potential at each MT sphere boundary, V_{MT}, are reported in Table 1. The final program of the procedure (an extension of that of Durham et al. 1982) calculates E // z and E // xy polarised XANES spectra and can handle clusters with no symmetry at all, as in our case. The unpolarised spectrum is obtained by a 2 : 1 weighted sum of the E // xy and E // z spectra.

The clusters used for the MS simulations include 32 atoms from the porphyrin ring, the proximal histidine and the CO ligand, with the central Fe atom, and a first shell including 4 pyrrolic nitrogens Np at 2.01 Å for MbCO and 2.06 Å for Mb (from EXAFS, as indicated above). The Fe atom was put in the heme plane in MbCO, while in Mb it was 0.45 Å out of the heme plane, towards the proximal histidine. In MbCO the C atom of the CO molecule was put at 1.97 Å, with an angle Fe–C–O of 150 deg. The distance (Fe–N_ε) of the proximal histidine nitrogen was 2.1 Å in Mb and 2.3 Å in MbCO. The residual coordinates come from crystallographic data (Mb from Takano 1977, and MbCO from Kuriyan et al. 1986). A sketch of the structures is shown in Fig. 1.

Results

By the dispersive technique, we measured directly the difference spectrum between the photo product Mb* and MbCO in a temperature range between 15 K and 100 K under continuous illumination. In order to interpret the spectrum, it is necessary to refer to the same difference spectrum between the two equilibrium forms Mb and MbCO.

The difference spectrum Mb*–MbCO at 30 K, in Fig. 2, panel A, shows the same minima and maxima as the spectrum of Mb–MbCO shown in panel B (solid line), in which we compare the XANES spectra of the equilibrium forms MbCO (dotted curve) and Mb (dashed curve). As is clear from the bottom figure, positive peaks in the difference spectrum correspond to peaks in the Mb spectrum (A′, A, D, D′ and E), whereas negative peaks correspond to peaks of the MbCO spectrum (C_1 and C_2). The peaks C_1 and C_2 are due to focusing scattering on the Fe–C–O–Fe photoelectron pathway (Bianconi 1985 b), while the peaks D and D′ originate from scattering on the heme plane and their intersities are expected to depend on heme doming effects in the dissociation process. The high energy region above 50 eV is called the Ligand Field Indicator Region (LFIR). The increase of LFIR between 50 eV and 60 eV has been related to Fe-heme displacement (Chance et al. 1986). The peak A in the difference spectrum Mb–MbCO corresponds to the energy red-shift of 2.5 eV of the absorption edge, going from MbCO to Mb. The amplitude of the peaks A′ and A in the Mb*–MbCO difference spectrum is about one half of the same peaks in the Mb–MbCO difference spectrum, indicating a lower red-shift of the absorption edge of Mb*, whose interpretation is difficult, because at least 3 terms are known to influence this feature (Bianconi et al. 1985 a): i) the change of the average first shell distance, ii) the change of the coordination number, and iii) the variation of the net charge at the Fe site.

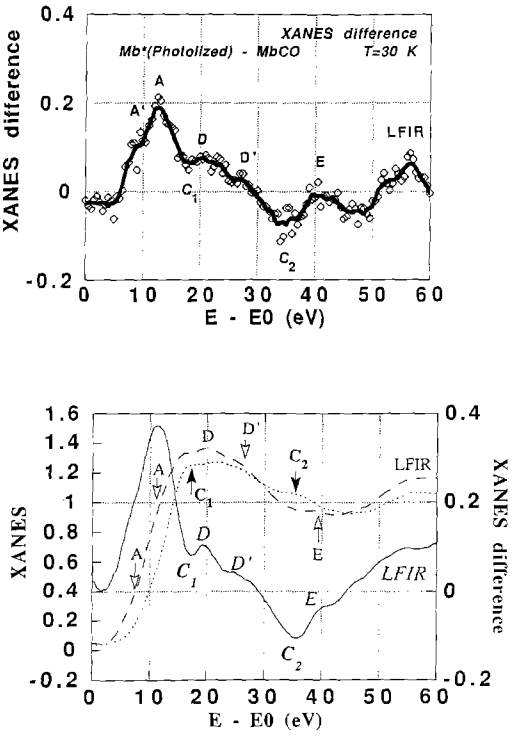

Fig. 2. *Lower panel. Solid line:* Fe K-edge XANES difference spectrum in sperm whale myoglobin [Mb–MbCO]. The spectra of Mb (*dashed curve*) and MbCO (*dotted curve*) are also reported. *Higher panel.* Fe K-edge XANES difference spectrum between the photoproduct and MbCO at 30 K. The energy zero corresponds to 7111.2 eV

In Fig. 3 the simulation of the ligand effect in the MS scheme is shown: the XANES calculations concern the equilibrium forms of Mb (dashed line) and MbCO (solid lines). The peaks C_1 and C_2 disappear as a result of removing the CO molecule from the atomic cluster (bottom curves, axial scattering). Moreover the MS theory predicts an energy red-shift of about 1.8 eV of the absorption threshold going from MbCO to Mb (upper curves, aver-

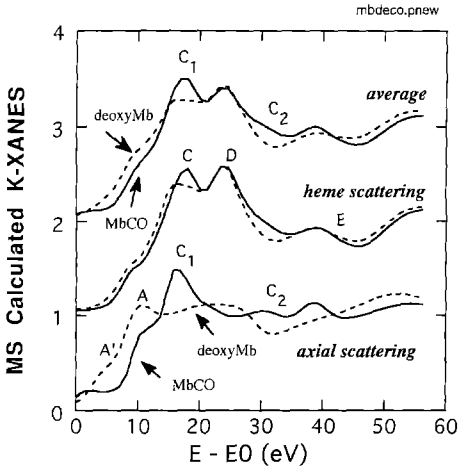

Fig. 3. Simulation of the ligand effect on the XANES spectrum of Mb: The MS XANES calculations of deoxy Mb (*dashed line*) and MbCO (*solid lines*) are superimposed. *Bottom curves:* scattering along the heme normal. *Central curves:* scattering in the heme plane. *Upper curves:* Averaged curves simulating the unpolarized absorption. The ability of the MS approach to calculate XANES spectra as a function of the size of the cluster and of the scattering orientation, allows one to extract structural information from the spectra. The peak A decreases with increasing the displacement Fe–Ct. At the same time the energy shift in the e // xy calculation increases

aged scattering), due both to the increase of the Fe–N_p distance after the out-of-plane movement of the iron (centre curves, heme scattering), and the increase of the density of quasi-atomic p-states (features A′ and A), as a consequence of removing the CO molecule (bottom curves, axial scattering). According to this scheme, the residual energy shift of 0.7 eV observed in the experimental XANES spectra is assigned to the reduction of the net charge at the iron site.

In Fig. 4 the XANES differences spectra photo product (T) – MbCO (15 K) at T = 15 K, 30 K, 40 K, 60 K, 80 K and 100 K under continuous illumination are shown. We

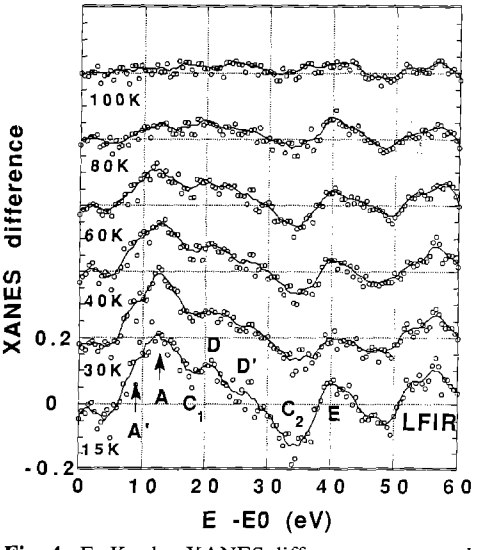

Fig. 4. Fe K-edge XANES difference spectrum between the photoproduct at different temperatures, under continuous illumination, and MbCO at 15 K. The temperatures reported are 15 K, 30 K, 40 K, 60 K, 80 K, 100 K

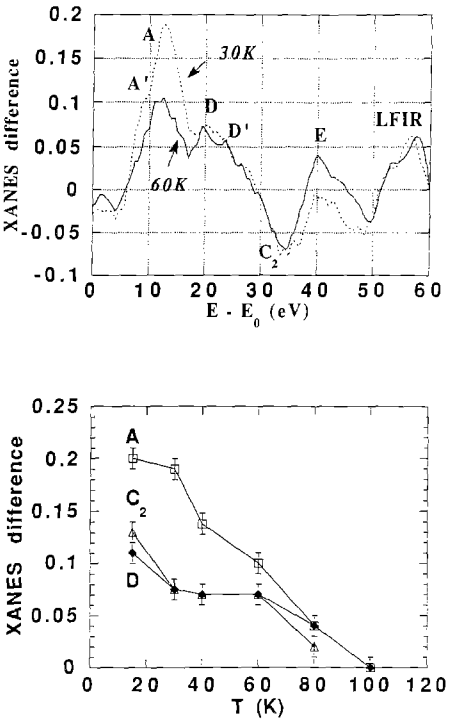

Fig. 5. *Lower panel:* temperature dependence of the peaks A, D, and C2 of the XANES difference spectrum between the photoproduct and MbCO. *Higher panel:* Superimposed XANES difference spectra of photoproduct. (30 K) – MbCO (15 K) and photoproduct (60 K) – MbCO (15 K)

used the same spectrum of MbCO (15 K) as a reference, to rule out the possibility that temperature effects on MbCO could influence the analysis of the data. The same features A′, A, C1, D, D′, C2 and E are always present, but the line shape of the spectrum changes with temperature. The intensity ratio between the peaks D and A is about 0.5 for T < 30 K, and about 0.8 for T > 50 K. Moreover the peak E at about 40 eV remains stronger than in the difference spectrum of the equilibrium forms over all the temperature range. The XANES difference in the LFI Region is always positive, confirming the displacement of the Fe from the heme plane. At 100 K the rebinding rate becomes faster than the acquisition time of the dispersive technique. In Fig. 5 the temperature dependence of the spectral difference peaks A, C_2, D in the lower panel, and the XANES difference spectra at 30 K and 60 K in the upper panel, are superimposed, demonstrating the spectral transition between these temperatures.

Discussion

Photoproduct at T < 30 K

From the preliminary analysis reported in the preceding section, the structure of the photoproduct Mb* at 30 K is unbound, with a structure similar to that of the equilibrium form of Mb. This XANES result is in contrast with the EXAFS data of Chance et al. (1983) which showed that the CO molecule in the photoproduct at very low temperature (4 K) remains very close to the iron, so it is necessary to explain why these two closely related techniques

give different results. It seems reasonable that, for example, owing to multiple scattering effects, the sensitivity of certain spectral features to a particular structural parameter could be different for XANES and EXAFS. The main XANES evidence for a 5-coordinated Fe out-of-plane in Mb* is the energy shift of the absorption edge (1.2 eV). This evidence is reinforced by the possibility of having underestimated difference data owing to a photolysis extent less than 100%. However, as regards the T > 50 K photoproduct (see below), if the CO molecule is 2.6 Å away from the Fe, as concluded by Powers et al. (1984), our result is not in conflict with it. Now we discuss in detail the structure of the photoproduct according to the XANES data.

Fe–N_p distance and Fe-heme displacement. The intensity of the peak A is related to the energy shift of the absorption edge. In the Mb*–MbCO difference spectrum it is 0.18, lower (≈50%) than in the difference spectrum between the equilibrium forms Mb–MbCO (0.37) that corresponds to a red-shift of 2.5 eV. Using a criterion of proportionality between the amplitude of the peak A, and the edge shfit, we measure 1.2 eV for the red-shift of the absorption edge in the photoproduct Mb*, of which 0.9 eV is the quantity assigned to structural effects. According to MS theory, this energy shift corresponds to a lengthening by 0.025 Å of the Fe–N_p distance. This estimation based on the criterion of proportionality leads to a good agreement with the value of d(Fe–N_p) = 2.03 found by EXAFS (Chance et al. 1983; Powers et al. 1984) for Mb*. However it can be altered if a non-linear variation of the Fe net charge, or partial photolysis, are considered (see the Results section). Considering a complete reduction of the Fe net charge after photolysis, or no reduction at all, the energy shifts assigend to structural effects become respectively 0.5 eV and 1.2 eV, giving a lengthening of the Fe–N_p of respectively 0.01 Å and 0.033 Å. The high energy part of the spectrum, LFIR, beyond 50 eV, increases, confirming that the Fe atom exits from the heme plane. Having no direct measure of the net charge effect, the XANES result is consistent with a position of the Fe atom out-of-plane by no more than 0.3 Å, intermediate between the carboxy- and the deoxy-configurations. A mechanism invoked to account for the out-of-plane movement of the Fe atom is the pseudo Jahn-Teller (PJT) effect (Bersuker and Stavrov 1988). According to the vibronic approach, after the breaking of the CO bond, the position of the five-fold coordinated iron site becomes unstable with respect to out-of-plane modes of A_{2u} symmetry, because of PJT coupling between the $a_{2u}(\pi)$ porphyrin orbital and the $d_{z2\text{-}\sigma}$ Fe–N_ε anti-bonding orbital.

Iron spin state. The XANES features above 5 eV probe delocalized unoccupied electron p-states, and not the electronic configuration of the d-states of the iron. The unoccupied d-states could be probed from the position and intensity of two little pre-peaks P and P′ at about 0 eV (not noted in our figures), that are interpreted as dipole forbidden 1s → 3d transitions, but their changes are too weak to be visible in the difference spectrum. However, other XANES features have been empirically related to the iron spin state. In Fig. 6, the derivative spectra of MbCO (solid curve) and Mb (dashed curve) are presented, together with the derivative of the spectrum obtained by the sum MbCO + (Mb*–MbCO), which should give the Mb* spectrum on assuming 100% photolysis extent. The shape of the derivative spectrum at the edge region is sensitive to the iron spin state (Oyanagy 1987): LS Fe(II) MbCO has a narrow absorption edge (FWHM = 3.4 eV at the peak at 13 eV of the derivative spectrum), while HS (Fe(II) Mb has a larger peak (FWHM = 6.5 eV at about 10 eV). Our reconstructed Mb* derivative spectrum has an FWHM of about 5.5 eV at the peak at about 12 eV, indicating a transition to an intermediate $(d_\pi)^3$, $(d_{xy})^1$, $(d_{z2})^1$, or HS $(d_\pi)^2$, $(d_{xy})^1$, $(d_{z2})^1$, $(d_{x2-y2})^1$ configuration of the iron. For an intermediate Fe spin state, a minor displacement with respect to the (deoxy-like) HS state is predicted in the frame of the vibronic approach; according to magnetic susceptibility data (Roder et al. 1984); however, the iron in Mb* at T > 5 K should be in a HS state, magnetically indistinguishable from Mb.

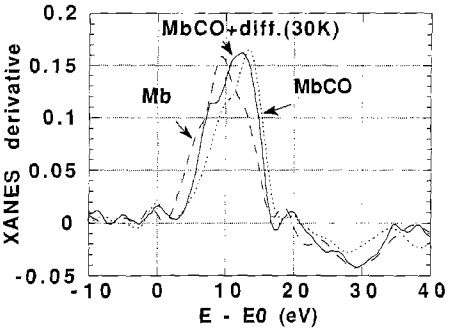

Fig. 6. XANES derivative spectrum of MbCO (*dotted curve*) and Mb (*dashed curve*) obtained by standard XANES scanning mode. The solid curve represents the derivative spectrum of MbCO + (Mb* – MbCO), obtained by summing the dispersive XANES difference between the photoproduct and MbCO at 30 K to the MbCO spectrum

Fe-His distance. Recently a peak between 5 and 10 eV of the edge region of the XANES spectrum has been suggested as a probe of the Fe–N_ε distance in the six-fold coordinated Fe site of dromedary nitrosyl-hemoglobin (Congiu Castellano et al. 1991). A similar trend is predicted from MS simulations on the five-fold coordinated Fe site in deoxy-myoglobin: a red shift of the peak A should be related to the elongation of the Fe–N_ε distance (Della Longa, unpublished observation). This information requires a very careful analysis of the region between the peaks A′ and A, and the expected changes for a variation of 0.1 Å are within 2–3% of the absorption jump, within the limits of the errors of our difference data. Hence no significant variation of the Fe–N_ε distance can be inferred from this experiment.

Photoproduct at T > 50 K

We observed changes in the XANES difference photoproduct (T) – MbCO (15 K) spectrum on increasing the temperature under continuous illumination (Fig. 4). The overall intensity of the difference spectrum decreases because

of the increasing rate of CO rebinding (Austin et al. 1975) but we observe a non rigid decrease of the various features. The peaks A and A′ decrease markedly while the peaks D and D′ exhibit small variations in the temperature range between 30 K and 60 K. These changes obviously reflect the changes in the absorption spectrum of the photoproduct (T), because the same MbCO (15 K) spectrum is always subtracted. The changes of the line shape of the XANES spectrum can be explained by assuming that two main substates of sperm whale Mb* exist at low temperature, with two different rebinding rate coefficients. Because inhomogeneity of myoglobin at low temperature is an accepted idea, they should be related to two MbCO substates at low temperature.

We use the ratio D/A to identify the two states, being D/A=0.5 for the faster state Mb* below 30 K, and D/A=0.8 for the slower Mb** above 50 K. As shown above, the intensity of peak A reflects the lengthening of the Fe–N_p distance due to the Fe-heme displacement (see Fig. 2 panel b). According to MS theory (Fig. 3, centre curves), and to polarised experiments on a MbCO crystal (Bianconi et al. 1985 b), the peaks D and D′ are due to heme scattering, hence changes in the intensity of the D and D′ peaks should reflect doming effects, i.e. distortions of the heme plane. Experimental evidence of such a correlation has been reported for the 'basket-handle' Fe(II) CO bound porphyririns (Cartier et al. 1992): the intensity of peak D increases with the distortion of the tetrapyrrolic macrocycle owing to the shortening of the basket handle side chain.

A structural mechanism related to this spectral transition includes an Fe atom slightly closer to the averaged plane of the pyrrolic nitrogens in the slower state (determining a slower energy shift of the edge), and/or distortions of the heme plane (enhancing the value of D and in turn the ratio D/A).

Doming effects. Doming effects should play an important role in the mechanism of the ligand binding to the iron site of the protein. As proposed by Doster (1989 b) the existence of two intermediate deoxy-like states, one of which is faster, with an almost planar heme geometry, could explain the fact that the non adiabatic binding of CO is faster than predicted, and similar to the average speed of O_2 binding, that should associate adiabatically. The conformational landscape of the low temperature photoproduct emerging from our experiments includes a faster state Mb* with an almost planar (carboxy-like) heme and a little Fe-heme displacement, and a slower Mb** state with a distorted heme. In the previous discussion on the PJT effect, a D_{4h} point group symmetry of the porphyrin plane, and a C_{4v} symmetry of the Fe-heme system after photolysis were assumed. However, owing to the strains from peripheral substituents and protein-heme contact, distortions with A_{1g}-, B_{1g}- and A_{2g}-type symmetry (Gouterman 1979), coupled with perturbations localised at specific pyrrolic nitrogens and carbons are accessible to the porphyrin ring, as shown by experiments on the depolarisation ratio and resonance excitation profiles of the Raman line ν_4 (Schweitzer-Stenner and Dreybrodt 1992). Hence vibrational modes of opportune symmetries can promote heme transitions between planar and domed conformations. The energy difference between these conformational minima, extracted from this XANES experiment, should be very small (about 30 cm^{-1}). This value is within the frequency range observed in the structure sensitive heme macrocycle vibrational modes (for example band I: 1 340–1 390 cm^{-1}, band II: 1 470–1 505 cm^{-1}). At T<30 K, another possibility is that the strain determined by the out-of-plane movement of the iron after photolysis would be stronger to the heme, in a protein matrix maintained in a CO-form that contacts the heme more closely than in the deoxy-form (although the distal pocket in MbCO is larger than in Mb, 90 Van der Waals contacts in MbCO against 74 in Mb are reported by crystallography; Takano 1977).

It should be noted that in the binding mechanism proposed by Doster the protein matrix should have the overall configuration of Mb, and not of MbCO, hence the structure determined by this XANES experiment could be not directly related to the mechanism giving fast binding of CO to myoglobin. However, it is likely that the presence of the ligand in the heme pocket is the first step for the conformational transition of the iron site in a CO-like form, with a more planar porphyrin ring, that in turn accelerates the average speed of binding.

Summary

In summary, a structural model of the intermediate states of myoglobin can be inferred for the photodissociation process at low temperature; when the light strikes the Fe site at low temperature the CO moves away, remaining in the heme pocket. An iron spin transition takes place, to an intermediate or HS configuration, causing the out-of-plane movement of the iron atom, through PJT coupling between the $a_{2u}(\pi)$ porphyrin orbitals and the $d_{z2-\sigma}$ Fe–N_ε anti-bonding orbital. The average distance Fe–N_p should be 2.03 Å, consistent with EXAFS and Raman data. At temperatures below 30 K, the conformation with the highest probability has a planar heme moiety, frozen in a MbCO-like form: this is the faster state Mb*. At temperatures above 50 K, a slower domed conformation Mb** is revealed under extended illumination. The equilibrium between the populations of these two different main substates determines the kinetics of the reassociation from the heme pocket at very low temperature. Both of these states are different from the equilibrium deoxy-form Mb of the protein, when the CO molecule has moved away from the heme pocket. A further mechanism relating the exit of the CO molecule, protein relaxation, and structural modification of the iron site (via the proximal histidine, and/or heme Van der Waals contacts) is necessary to assume the definitive, equilibrium structure.

Acknowledgement. This work was supported by a grant from GNCB-CNR, Italy and by EC's LIP programme.

References

Amiconi G, Santucci R, Coletta M, Congiu Castellano A, Giovannelli A, Dell'Ariccia M, Della Longa S, Barteri M, Burattini E, Bianconi A (1989) Influence of globin structure on the heme in dromedary carbonmonoxyhemoglobin. Biochemistry 28: 8547–8553

Antonini E, Brunori M (1971) Hemoglobin and myoglobin in their reactions with ligand. North-Holland, London

Ascone I, Fontaine A, Bianconi A, Congiu Castellano A, Giovannelli A, Della Longa S, Momentau M (1987) Energy dispersive X-ray Absorption Spectroscopy: strenghts and limitations for time resolved studies of biostructures. In: Bianconi A, Congiu Castellano A (eds) Biophysics and Synchrotron Radiation. Springer series in Biophysics, vol. 2. Springer, Berlin Heidelberg New York, pp 202–211

Austin RH, Benson KW, Eisenstein L, Frauenfelder H, Gunsalus IC (1975) Dynamics of ligand binding to myoglobin. Biochemistry 14: 5355–5373

Bersuker IB, Stavrov SS (1988) Structure and properties of metalloporphyrins and hemoproteins: the vibronic approach. Coord Chem Rev 88: 1–68

Bianconi A, Congiu Castellano A, Dell'Ariccia M, Giovannelli A, Burattini E, Durham PJ (1985 a) Increase of the effective charge in hemoproteins during oxygenation process. Biochem Biophys Res Commun 131: 98–102

Bianconi A, Congiu Castellano A, Durham PJ, Hasnain SS, Phillips S (1985 b) The CO bond angle of carboxymyoglobin determined by angular-resolved XANES spectroscopy. Nature 318: 685–687

Cartier C, Momenteau M, Dartyge E, Fontaine A, Tourillon G, Bianconi A, Verdaguer M (1992) X-ray absorption spectroscopy of carbonyl basket-handle Fe(II) porphyrins: the distortion of the tetrapyrrolic macrocycle. Biochim Biophys Acta 1119: 169–174

Chance B, Fischetti R, Powers L (1983) Structure and kinetic of the photoproduct of MbCO at low temperature: an X-ray absorption study. Biochemistry 22: 3820–3829

Chance B, Powers L, Kumar C, Chance B (1986) X-ray absorption studies of myoglobin peroxide reveal functional difference between globins and heme enzymes. Biochemistry 25: 1259–1265

Congiu Castellano A, Della Longa S, Bianconi A, Barteri M, Burattini E, Amiconi G, Ascenzi P, Coletta M, Santucci R (1991) Influence of allosteric effectors on the heme conformation of dromedary ferrous nitrosylhemoglobin detected by XANES spectroscopy. Biochim Biophys Acta 1080: 7–13

Della Longa S, Bianconi A, Palladoni L, Simonelli B, Congiu Castellano A, Borghi E, Barteri M, Beltramini M, Rocco GP, Salvato B, Bubacco L, Magliozzo RS, Peisach J (1993) A XANES study of metal coordination in Co(II)-substituted Carcinus maenas hemocyanin. Biophys J 65: 2680–2691

Doster W (1989 b) On the mechanism of ligand binding to myoglobin. Eur Biophys J 17: 217–220

Doster W, Kusack S, Petry W (1989 a) Dynamic transition of myoglobin revealed by inelastic neutron scattering. Nature 337: 754–756

Durham P, Pendry JB, Hodges CH (1982) Calculation of X-ray absorption near edge structure, XANES. Comput Phys Commun 25: 193–200

Elber R, Karplus M (1987) Multiple conformational states of proteins: a molecular dynamics analysis of myoglobin. Science 235: 318–321

Fermi G, Perutz MF, Shaanan B, Fourme R (1981) The crystal structure of human deoxyhaemoglobin at 1.74 Å resolution. J Mol Biol 175: 159–174

Fiamingo FG, Alben JO (1985) Structures of photolyzed carboxymyoglobin. Biochemistry 24: 7964–7970

Fontaine A, Dartyge E, Itie JP, Jucha A, Polian A, Tolentino H, Tourillon G (1989) Time resolved X-ray absorption spectroscopy using an energy dispersive optics: strenghts and limitations. In: Topics in Current Chemistry, vol. 151. Springer, Berlin Heidelberg New York, pp 179–203

Frauenfelder H, Parak F, Young RD (1988) Conformationale substates in protein. Annu Rev Biophys Biophys Chem 17: 451–479

Gilch H, Schweitzer-Stenner R, Dreybrodt W (1993) Structural heterogeneity of the Fe^{2+}–Ne(HisF8) bond in various hemoglobin and myoglobin derivatives probed by the Raman-active iron histidine stretching mode. Biophys J 65: 1470–1485

Gouterman M (1979) In: The Porphyrins, vol. 3. Dolphin D (ed) Academic Press, New York, p 1

Hong MK, Braunstein D, Cowen BR, Frauenfelder H, Iben IET, Mourant JR, Ormos P, Scholl R, Schulte A, Steinbach PJ, Xie Y, Young RD (1990) Conformational substates and motions in myoglobin. Biophys J 58: 429–436

Iizuka T, Yamamoto H, Kotani M, Yonetani T (1974) Low temperature photodissociation of hemoproteins: carbon monoxide complex of myoglobin and hemoglobin. Biochim Biophys Acta 371: 126–139

Kuriyan J, Wilz S, Karplus M, Petsko GA (1986) X-ray structure and refinement of Carbon-monoxy (Fe II)-myoglobin at 1.5 Å resolution. J Mol Biol 192: 133–154

Li C, Pompa M, Della Longa S, Bianconi A (1991) Electronic structure of La_2CuO_4 joint analysis of O K and Cu K and L3 edge X-ray absorption spectra. Physica C 178: 421–431

Mills DM, Lewis A, Harootunian A, Huang J, Smith B (1984) Time-resolved X-ray absorption spectroscopy of carbonmonoxide-myoglobin recombination after laser photolysis. Science 223: 811–813

Moore JN, Hansen PA, Hochstrasser RM (1988) A new method for picosecond time-resolved infrared spectroscopy: applications to CO photodissociation from iron porphyrins. Proc Natl Acad Sci, USA 85: 5062–5066

Mourant JR, Braunstein DP, Chu K, Frauenfelder H, Nienhaus GU, Ormos P, Young RD (1993) Ligand binding to heme proteins: II. Transitions in the heme pocket of myoglobin. Biophys J 65: 1498–1507

Ormos P, Braunstein D, Frauenfelder H, Hong MK, Lin S, Sauke TB, Young RD (1988) Orientation of carbonmonoxide and structure-function relationships in carbonmonoxymyoglobin. Proc Natl Acad Sci, USA 85: 8492–8496

Oyanagy H, Iizuka T, Matsushita T, Saigo S, Makino R, Ishimura Y (1987) Local structure of heme-iron studied by high resolution XANES: thermal spin equilibrium in myoglobin. In: Biophysics and Synchrotron Radiation. Bianconi A, Congiu Castellano A (eds) Springer, New York, pp 99–196

Palladino L, Della Longa S, Reale A, Belli M, Scafati A, Onori G, Santucci A (1993) XANES of Cu(II)-ATP and related compounds in solution: quantitative determination of the distortion of the Cu site. J Chem Phys 98(4): 2720–2726

Parak F, Hartmann H, Aumann KD, Reuscher H, Rennekamp G, Bartunik H, Steigemann W (1987) Low temperature X-ray investigation of structural distributions in myoglobin. Eur Biophys J 15: 237–249

Phillips SEV (1981) X-ray Structure of Deoxy-Mb (pH 8.5) at 1.4 Å resolution. Brookhaven Protein Data Bank

Powers L, Sessler JL, Woolery GL, Chance B (1984) CO bond angle changes in photolysis of MbCO. Biochemistry 2: 5519–5523

Powers L, Chance B, Chance M, Campbell B, Khalid J, Kumar C, Naqui A, Reddy KS, Zhou Y (1987) Kinetic, structural and spectroscopic identification of geminate states of Mb: a ligand binding site of reaction pathway. Biochemistry 26: 4785–4796

Roder H, Berendzen J, Bowne SF, Frauenfelder H, Sauke TB, Shyamsunder E, Weissman B (1984) Comparison of the magnetic properties of deoxy- and photodissociated myoglobin. Proc Natl Acad Sci, USA 81: 2359–2363

Rousseau DL, Argade PV (1986) Metastable photoproducts from carbon monoxide myoglobin. Proc Natl Acad Sci, USA 83: 1310–1314

Sassaroli M, Rousseau DL (1986) Simulation of Carboxymyoglobin photodissociation. J Biol Chem 261: 16292–16294

Schweitzer-Stenner R, Dreybrodt W (1992) Investigation of haemprotein coupling and structural heterogeneity in myoglobin and haemoglobin by resonance Raman spectroscopy. J Raman Spectrosc 23: 539–550

Teng T, Huang HW, Olah GA (1987) 5 K EXAFS and 40 K 10-s resolved EXAFS studies of photolyzed MbCO. Biochemistry 26: 8066–8072

Takano T (1977) Structure of Myoglobin refined at 2.0 Å resolution. J Mol Biol 110: 569–584

Zhang K, Chance B, Reddy KS (1989) X-ray Absorption Near Edge Study of Mb and MbCO. Physica B 158: 121–122